

Research on Differential Tomography SAR Imaging of Urban Buildings -- Taking the Government Building in Bao'an District, Shenzhen as an Example

Jianxu Wang^{1*}, Long Li^{1,2}, Chonghui Zhang^{1,3}

1. School of Geomatics and Urban Spatial Informatics, Beijing University of Civil Engineering and Architecture, Beijing 102616, China.

2. Shandong Institute of Geological Survey and Mapping, Jinan 250002, Shandong, China.

3. Shandong General Team of China Building Materials Geological Exploration Center, Jinan 25000, Shandong, China.

*Corresponding author. Email address: 1248250014@qq.com

Abstract: Differential SAR Tomography (D-TomoSAR), an extension of InSAR technology, integrates D-InSAR and TomoSAR to achieve imaging in the height-deformation rate (s-v) domain. It resolves SAR imaging layover issues and retrieves the elevation and deformation rate of scatterers within a pixel. Using the Bao'an District Government Building in Shenzhen as an example, this study applies D-TomoSAR for four-dimensional urban building imaging. Based on Persistent Scatterer (PS) points, the experiment involves interferometric processing and PS point selection to obtain differential interferogram sequences and PS points. The Orthogonal Matching Pursuit (OMP) algorithm is employed for D-TomoSAR imaging, reconstructing elevation-deformation rate backscattering profiles. Theoretical analysis and case studies assess resolution and reconstruction performance. Compared to traditional InSAR, D-TomoSAR retains high resolution while significantly improving scatterer reconstruction accuracy, achieving precise urban building deformation estimation. This study highlights the potential of D-TomoSAR for large-scale urban deformation monitoring applications.

Key words: D-TomoSAR; PS; OMP; deformation

1. Introduction

With the rapid development of urban construction in China, the quality of urban buildings is of paramount importance as it determines the overall standard of urban construction. Problems in urban buildings can have catastrophic consequences for residents, making deformation monitoring an essential measure to ensure building safety. Deformation monitoring is indispensable in operational management and post-construction maintenance. It plays a critical role in the construction and operation of urban buildings, with deformation monitoring, analysis, and prediction forming key components of building safety assessments. Timely understanding of deformation patterns and accurate predictions can proactively address potential safety hazards, underscoring the significance of urban building deformation monitoring.

Traditional methods for urban building deformation monitoring include GPS measurements, leveling, and observation piles. These methods are generally suitable for monitoring specific points on a building. However, for monitoring entire

structures, traditional approaches often fall short due to the large monitoring area and long time periods required. Techniques like the Permanent Scatterer (PS)^[1] method and the Small Baseline Subset (SBAS) method, based on time-series multi-baseline InSAR, have significantly improved the precision and scope of deformation monitoring. Nevertheless, these methods rely on scatterers dominant within a pixel. In densely built urban areas, severe layover effects may occur, with multiple scatterers at different heights contributing signals to a single radar resolution cell. Without effectively separating these mixed signals, accurate deformation monitoring becomes unattainable.

To address the inability of traditional methods to resolve deformation parameters in high-resolution SAR data affected by layover effects, Differential SAR Tomography (D-TomoSAR) has been proposed. As an extension of InSAR technology, D-TomoSAR integrates D-InSAR and TomoSAR techniques^[2] to achieve imaging in the height-deformation rate ($s-v$) domain. Using N registered SAR images, this technique reconstructs the scatterer distribution in the $s-v$ domain based on pixel amplitude and interferometric phase information through specific algorithms. It not only resolves SAR imaging layover issues but also retrieves the elevation and deformation rate of individual scatterers within a pixel. D-TomoSAR is primarily applied to complex urban scenarios with severe layover problems.

In this study, a signal model is established based on PS points. Interferometric processing and PS point selection are performed to obtain differential interferogram sequences and PS points in the study area. Due to the ability of Orthogonal Matching Pursuit (OMP) algorithm to compute least-squares solutions that minimize residuals and achieve high-precision signal reconstruction, this study employs the OMP^[3] algorithm for D-TomoSAR imaging. This enables the reconstruction of backscattering profiles in the elevation-deformation rate domain. Using a dataset of 36 TerraSAR-X images with one-meter resolution, deformation monitoring of the Bao'an District Government Building in Shenzhen, China, was conducted. Theoretical analysis and case studies were performed to evaluate resolution and reconstruction performance. Comparative experiments with traditional InSAR methods demonstrated that D-TomoSAR retains high-resolution advantages while significantly improving scatterer reconstruction accuracy, achieving high-precision deformation estimates for buildings. This study explores the application of D-TomoSAR in urban buildings, aiming to provide insights and references for its large-scale application in urban deformation monitoring in the future.

2. Study Area Data and Preprocessing

2.1 Study area data

The SAR dataset used in this experiment was obtained from the spaceborne TerraSAR-X platform, which features high-resolution and wide-swath imaging capabilities. The operating band is the X-band, and the initial SAR image data is in .xml format. Using the SAR preprocessing software Gamma, the format can be converted to .slc (Single Look Complex, SLC). Details of the SAR data are shown in Table 1.

Table 1. Overview of experimental data in this chapter

Project	Content
Data source	TerraSAR-X
Imaging mode	Stripmap, Descending orbit
Polarization mode	HH
Number of scenes	36
Coverage	Bao'an District Transportation Bureau Bao'an Management Bureau
Time span	2014.11-2017.11
Wave length	0.031 m
Incident angle	35.410°
Center slant distance (main image)	613670.036468

2.2 Preprocessing

Data preprocessing mainly includes the selection of a super master^[4] image, image co-registration and cropping, spatial and temporal baseline estimation, spatiotemporal baseline optimization, and amplitude calibration. The super master image is typically selected as the one located at the center of the temporal and spatial baselines to minimize spatial and temporal decorrelation effects, ensuring the quality of the interferograms. Image co-registration is performed by fitting a polynomial based on intensity cross-correlation information, achieving a registration accuracy of 0.01 pixels in the study area of the Shenzhen Bao'an District Government Building. When cropping the images, it is essential to ensure full coverage of the study area. Figure 1 shows the intensity map of the master image and the corresponding optical remote sensing image of the Shenzhen Bao'an District Government Building.

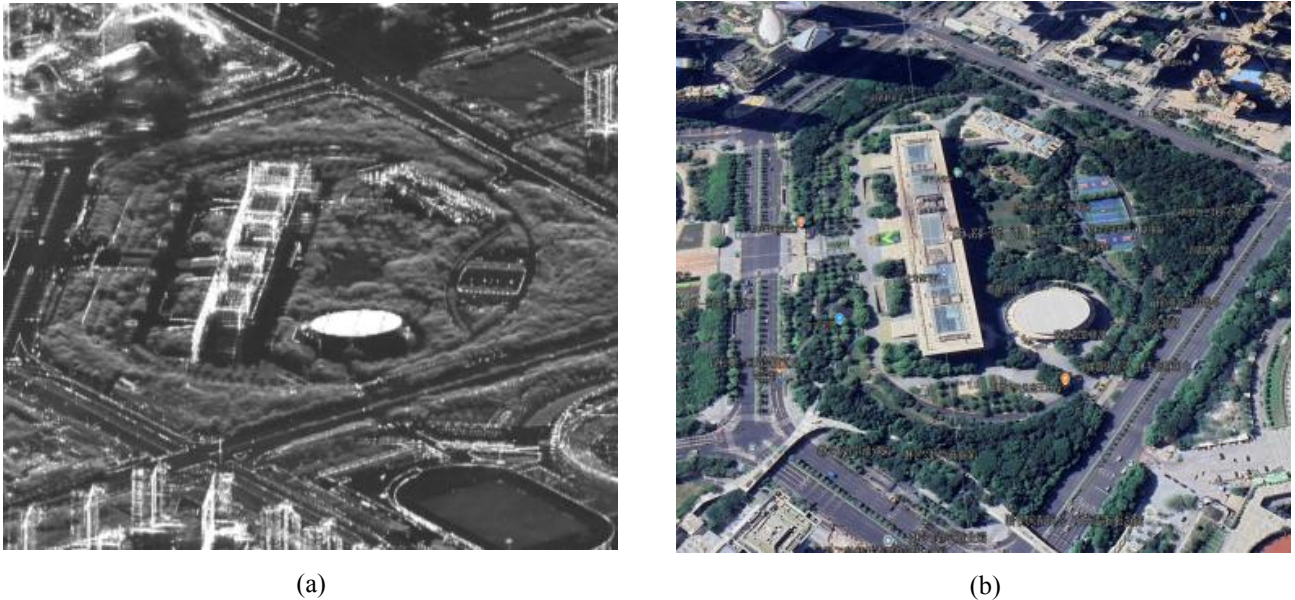


Figure 1. (a) SAR image of the research area, (b) Optical imaging of the research area.

The spatiotemporal baseline estimation utilizes high-precision satellite orbit data to calculate the vertical baselines between each auxiliary image and the main image. The time baseline is calculated based on the acquisition date and converted to years.

3. Experiment Steps of D-TomoSar

3.1 D-TomoSAR system mode

D-TomoSAR is a high-resolution ground target monitoring method based on synthetic aperture radar (SAR) technology, mainly used to achieve accurate reconstruction and deformation monitoring of multi-dimensional spatiotemporal scenes. This technology combines the advantages of SAR tomographic imaging (TomoSAR)^[5] and differential interferometric SAR (D-InSAR), and can extract accurate three-dimensional geometric structure information and time-series deformation information in complex environments, solving the problem of scatterer overlap in high-resolution SAR images.

Assume that a dataset of M single-look complex (SLC) SAR images^[6] has been obtained from the same region at different times and spatial positions. After performing two-dimensional compression in the azimuth-range direction, M single-look complex SAR images are obtained. One image, with spatial and temporal baselines near the center, is selected as the master image. The other images are registered and deslanted with respect to the master image, resulting in a sequence of complex values for each azimuth-range resolution cell, represented as

$$g_m = \int_{-s_{max}}^{s_{max}} c(s) \exp\left(j \frac{4\pi b_m}{\lambda r} s\right) \exp(j\varphi_m) ds \quad (1)$$

$$m = 1, 2, \dots, M$$

In the formula, $[-s_{max}, s_{max}]$ is the vertical span of the slant distance; $c(s)$ is the radar scattering characteristic function of the target; φ_m is the deformation phase of the slant range deformation rate at the tomographic sampling point. Under the linear deformation rate model $\varphi_m = -\frac{4\pi}{\lambda} t_m v(s)$, Let $\xi_m = \frac{2b_m}{\lambda r}$, $\eta_m = \frac{2t_m}{\lambda}$, $\gamma(s, v) = c(s)\delta(v - v(s))$, Then equation (1) can be written as follows

$$g_m = \int_{-s_{max}}^{s_{max}} \int_{-v_{max}}^{v_{max}} c(s, v) \exp(j2\pi\xi_m s) \exp(j2\pi\eta_m v) ds dv \quad (2)$$

$$m = 1, 2, \dots, M$$

In the formula, $[v_{-max}, v_{max}]$ is the deformation rate span; ξ_m and η_m are spatial frequency and temporal frequency respectively; v is the slope deformation rate to the sampling point; $\delta(v - v(s))$ is the Dirac function. According to formula (2), the D-TomoSAR observation data is expressed as a two-dimensional joint spectrum of the radar scattering characteristic function in the height direction and the deformation rate direction. Through a specific imaging algorithm, the scattering function value of the target signal is inverted, and the height position and deformation rate of the scattering point in the tomographic direction are determined according to the position of these function values, and finally the four-dimensional imaging of the target is realized.

3.2 Interference processing and PS point selection

First, interferometric processing is performed. Each cropped image in the study area is interfered with the master image to generate an interferogram sequence. Then, external DEM data are introduced for geocoding, transforming them into the SAR coordinate system and registering them with the images. Finally, using the geocoded DEM and orbital parameter information, a simulated terrain phase is generated, resulting in a differential interferogram sequence with the terrain and flat-earth phases removed.

The selection of PS points is crucial as it is a key step in the differential SAR tomography process. By selecting PS points, low coherence regions can be avoided, effectively solving the problem of spatial and temporal decoherence. This experiment mainly uses the amplitude deviation index method to select PS points. It mainly uses the statistical distribution of amplitude to select stable PS points, and selects PS points by analyzing the time series of echo amplitude composition. The main rule is to select points with larger MSR values, where $MSR = \frac{\mu}{\sigma}$, where μ and σ are the amplitude mean and standard deviation of each pixel in N SAR images, respectively. The amplitude deviation index method is simple to calculate and suitable for processing multi-scene image data and block processing of large data.

3.3 Compressive sensing

This paper uses the orthogonal matching pursuit (OMP)^[7] algorithm in compressed sensing technology to reconstruct two-dimensional signals. As a greedy algorithm, OMP is specifically used for the reconstruction of sparse signals and has been widely used in the fields of sparse representation theory and compressed sensing (CS). The algorithm mainly approximates sparse signals through redundant dictionaries or overcomplete bases, thereby effectively improving the accuracy and efficiency of signal reconstruction.

(1) Input matrix and the number of variables to be selected. Initialize residual, orthogonal projection matrix, subspace index set, and restore signal.

(2) Calculate $i = \operatorname{argmax}_i |A_i^T r_k|$, put i into the set S , that is, $S = S \cup \{i\}$.

(3) Calculate $P_k = A_S (A_S^T A_S)^{-1} A_S^T$, $r_k = (I - P_k)b$.

(4) Repeat steps 2 and 3 k times.

(5) Calculate $x_s = (A_s^T A_s)^{-1} A_s^T b$, get the value of the element at the corresponding position S in x .

(6) Return x .

4. Result and Analysis

In order to verify the applicability and accuracy of the proposed differential tomography four-dimensional imaging method, this paper conducted differential SAR tomography on the government building in Bao'an District, Shenzhen (detailed information such as high-resolution dataset and satellite parameter information, incident angle and slant range of each data, spatiotemporal baseline and resolution are shown in section 2.1). Figure 2 shows the deformation monitoring results of the government building in Bao'an District, Shenzhen. From the deformation rate chart, it can be seen that the deformation rate of the government building is roughly between -0.5 mm and 0.5 mm, indicating that the building has no significant deformation and is in a very stable deformation environment. Meanwhile, we also observed that the deformation rate of some scatterers at the bottom of the building exceeded -0.5 mm. This may be due to the influence of seasonal changes and temperature factors such as sunlight on some buildings around the bottom of the building, leading to thermal expansion and contraction, resulting in slight settlement. Although these changes exist, they are not sufficient to have a significant impact on the overall structural health of the building.

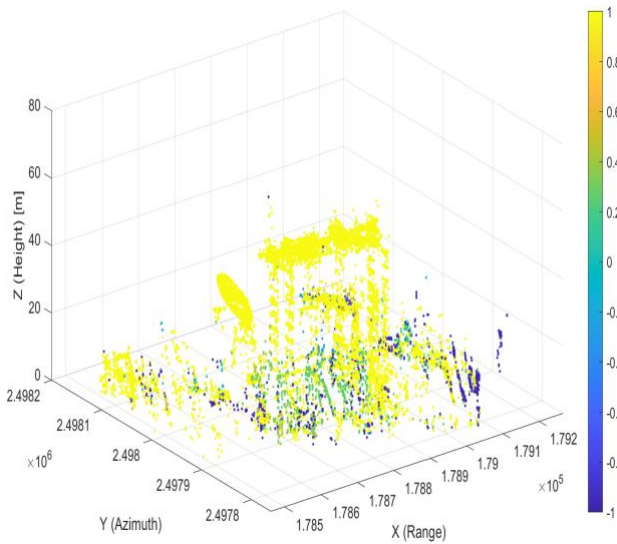


Figure 2. Four-dimensional deformation rate diagram.

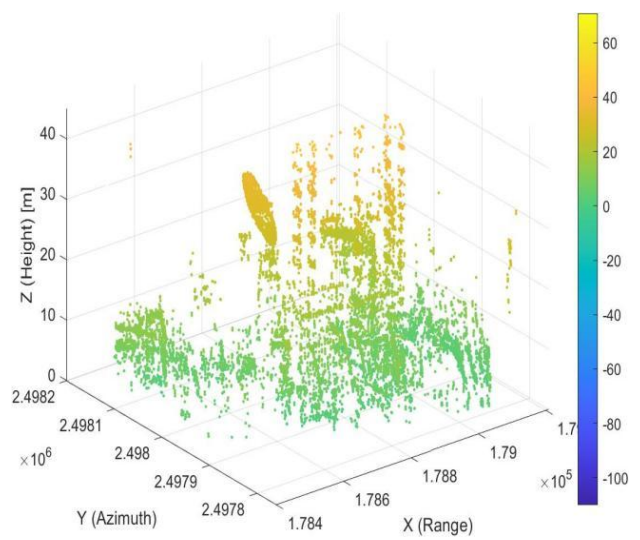


Figure 3. Three-dimensional elevation map.

From the three-dimensional point cloud map, the height of the Traffic Management Bureau is about 42 meters. By consulting the data, we know that the actual height of the building is about 45 meters, which proves that the elevation reconstruction results obtained through differential tomography experiments are relatively accurate. The top view in Figure 4 clearly shows the structural features of the government building, which can provide reference for future structural design and monitoring of government buildings. It is particularly noteworthy that the area we cropped in the experiment was not only the government building, but also the streets and other buildings in the surrounding area. The D-TomoSAR experiment also clearly reflects the elevation and deformation of these small areas. Therefore, this detail not only enhances the three-dimensional sense of the image, but also provides a solid foundation for our structural analysis of the government building.

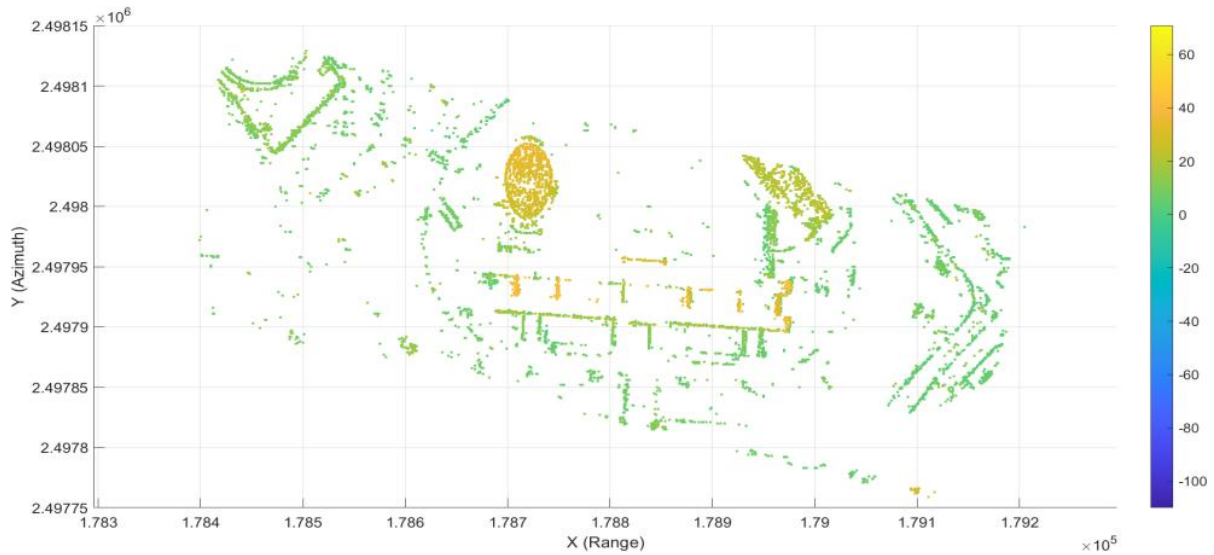


Figure 4. 3D elevation view.

5. Conclusion

This article is based on advanced D-TomoSAR technology, focusing on the field of urban building deformation monitoring, and striving to explore the potential and value of D-TomoSAR technology in the field of building monitoring. This article mainly uses Matlab to implement the D-TomoSAR algorithm, and conducts detailed research on the government building in Bao'an District, Shenzhen using 36 scenes of TerraSAR real data, verifying the high practical value of D-TomoSAR technology in deformation monitoring. The experimental exploration of government buildings shows that the overall deformation of the building is relatively stable, and each structural part is relatively healthy. This article provides reference for the further application of D-TomoSAR technology in the field of urban building deformation monitoring in the future. However, there are also some shortcomings in this study. Firstly, the SAR side view imaging mechanism results in missing information on the back of the antenna. In the future, a method combining lift orbit data can be considered to compensate for the current shortcomings and provide more comprehensive deformation monitoring of buildings in all directions; Secondly, the current obtained deformation information of government buildings is limited to the line of sight direction, which is only a component of the real deformation of the building and cannot comprehensively obtain the deformation information of the building. In the future, mathematical modeling, numerical simulation and other research on the real three-dimensional deformation information of ground objects can be considered.

Conflicts of Interest

The author declares no conflicts of interest regarding the publication of this paper.

References

- [1] Bekaert DPS, Walters RJ, Wright TJ, et. 2015. Statistical comparison of InSAR tropospheric correction techniques. *Remote Sensing of Environment*, 170: 40-47. DOI:10.1016/j.rse.2015.08.035.
- [2] Lombardini F. 2005. Differential tomography: a new framework for SAR interferometry. *IEEE Transactions on Geoscience and Remote Sensing*, 43(1): 37-44. DOI:10.1109/TGRS.2004.838371.
- [3] Pang L, Gai Y, Zhang T. 2021. Joint sparsity for TomoSAR Imaging in urban areas using building POI and TerraSAR-X staring spotlight data. *Sensors*, 21(20): 6888. DOI:10.3390/s21206888.
- [4] A new algorithm for surface deformation monitoring based on small baseline differential SAR interferograms |IEEE Journals & Magazine| IEEE Xplore[EB/OL]. [2024-11-23]. <https://ieeexplore.ieee.org/abstract/document/1166596>.

[5] Single-look multi-master sar tomography: an introduction |IEEE Journals & Magazine| IEEE Xplore[EB/OL]. [2024-11-23]. <https://ieeexplore.ieee.org/abstract/document/9133203>.

[6] Four-dimensional SAR imaging for height estimation and monitoring of single and double scatterers |IEEE Journals & Magazine| IEEE Xplore[EB/OL]. [2024-11-23]. <https://ieeexplore.ieee.org/abstract/document/4685869>.

[7] Montazeri S, Zhu XX, Eineder M, et al. 2016. Three-dimensional deformation monitoring of urban infrastructure by tomographic SAR using multitrack TerraSAR-X data stacks. *IEEE Transactions on Geoscience and Remote Sensing*, 54(12): 6868-6878. DOI:10.1109/TGRS.2016.2585741.